

Supporting Information

Table S1. Comparison of H₂S sensing properties of the CuO-functionalized SnO₂ nanowires with those of previous reports.^{14,18-20, 26-31}

Materials type	H ₂ S (ppm)	Response (R_a/R_g)	Response time (s)	Recovery time (s)	Operating Temp. (°C)	Ref.
CuO-functionalized SnO₂ nanowires	0.1–1	10–15	9	8	300	this work
CuO-loaded SnO₂ film	50	2.5×10^4	80	100	200	14
SnO₂-CuO-SnO₂ multilayer thick film	50	210	45	41	90	18
Cu-doped SnO₂ thin film	1000	910	10	1500	200	19
CuO-modified SnO₂ nanoribbons	3	180	15	.	27	20
CuO-doped SnO₂ thin film	50	3.6×10^5	600	180	150	26
SnO₂-ZnO-CuO composite thick film	50	6×10^4	15	420–480	250	27
CuO-SnO₂ core/shell nanorods	10	9.4×10^4	.	.	60	28
Cu-doped SnO₂ nanowires	50	6×10^6	.	.	150	29
CuO-doped SnO₂ nanowires	20	809	1	332	300	30
CuO-loaded SnO₂ nanofibers	10	1.98×10^4	1	10	300	31

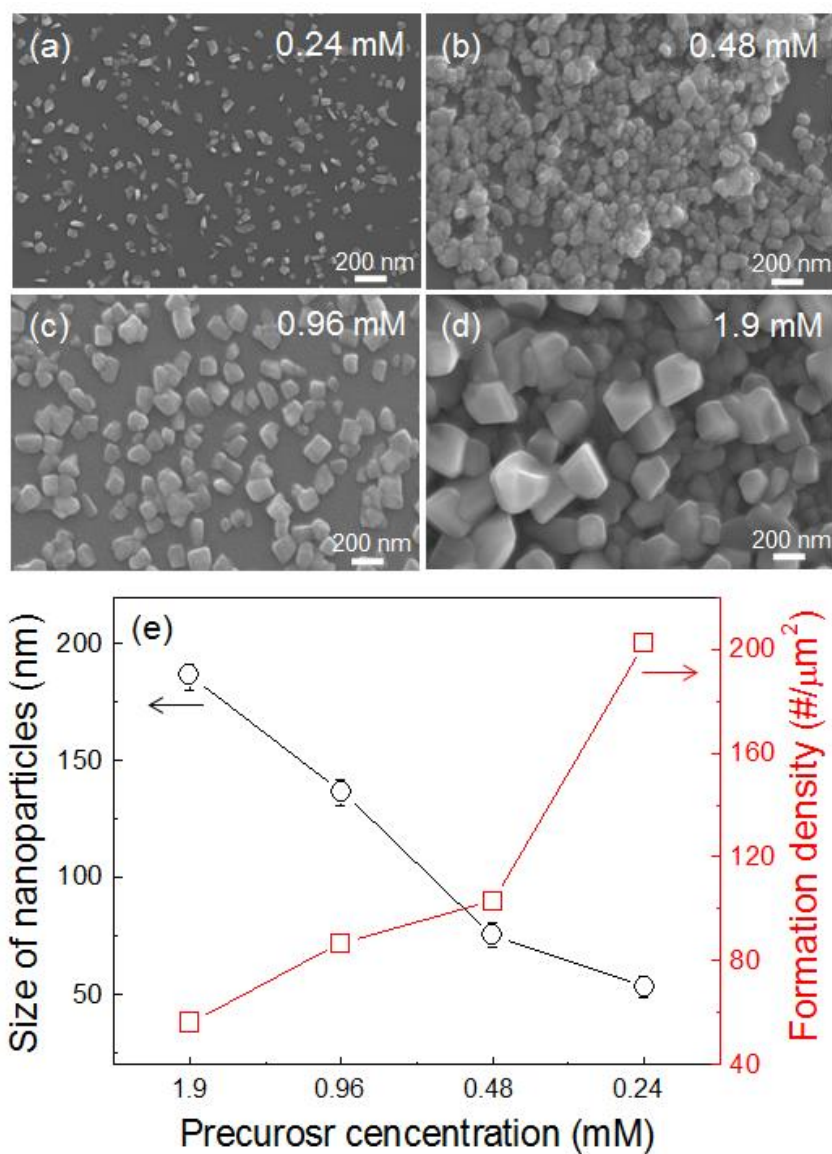


Fig. S1. Microstructures of Cu nanoparticles synthesized with different $\text{CuSO}_4 \cdot 5\text{H}_2\text{O}$ precursor concentrations in γ -ray radiolysis at $10\text{Gy}\cdot\text{h}^{-1}$ for 2h: (a) 0.24, (b) 0.48, (c) 0.96, and (d) 1.9 mM $\text{CuSO}_4 \cdot 5\text{H}_2\text{O}$ in a mixed solvent of deionized water (77 vol%) and 2- propanol (23 vol%). (e) The size and formation density of Cu nanoparticles summarized from the microstructures in (a)–(d).

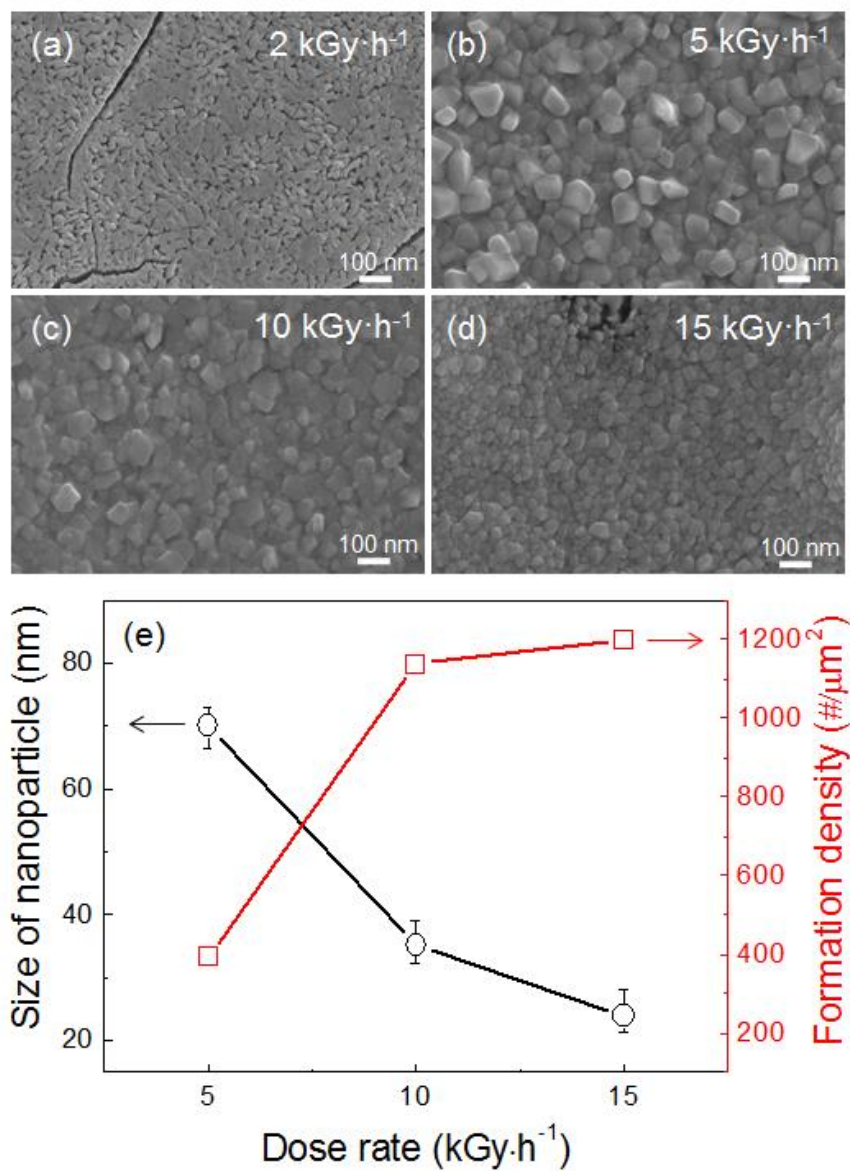


Fig. S2. Microstructures of Cu nanoparticles synthesized at various dose rates for 2 h at 0.96 mM CuSO₄·5H₂O : (a) 2, (b) 5, (c) 10, and (d) 15 kGy·h⁻¹ dose rate.(e) The size and formation density of Cu nanoparticles summarized from the microstructures in (c)–(d).

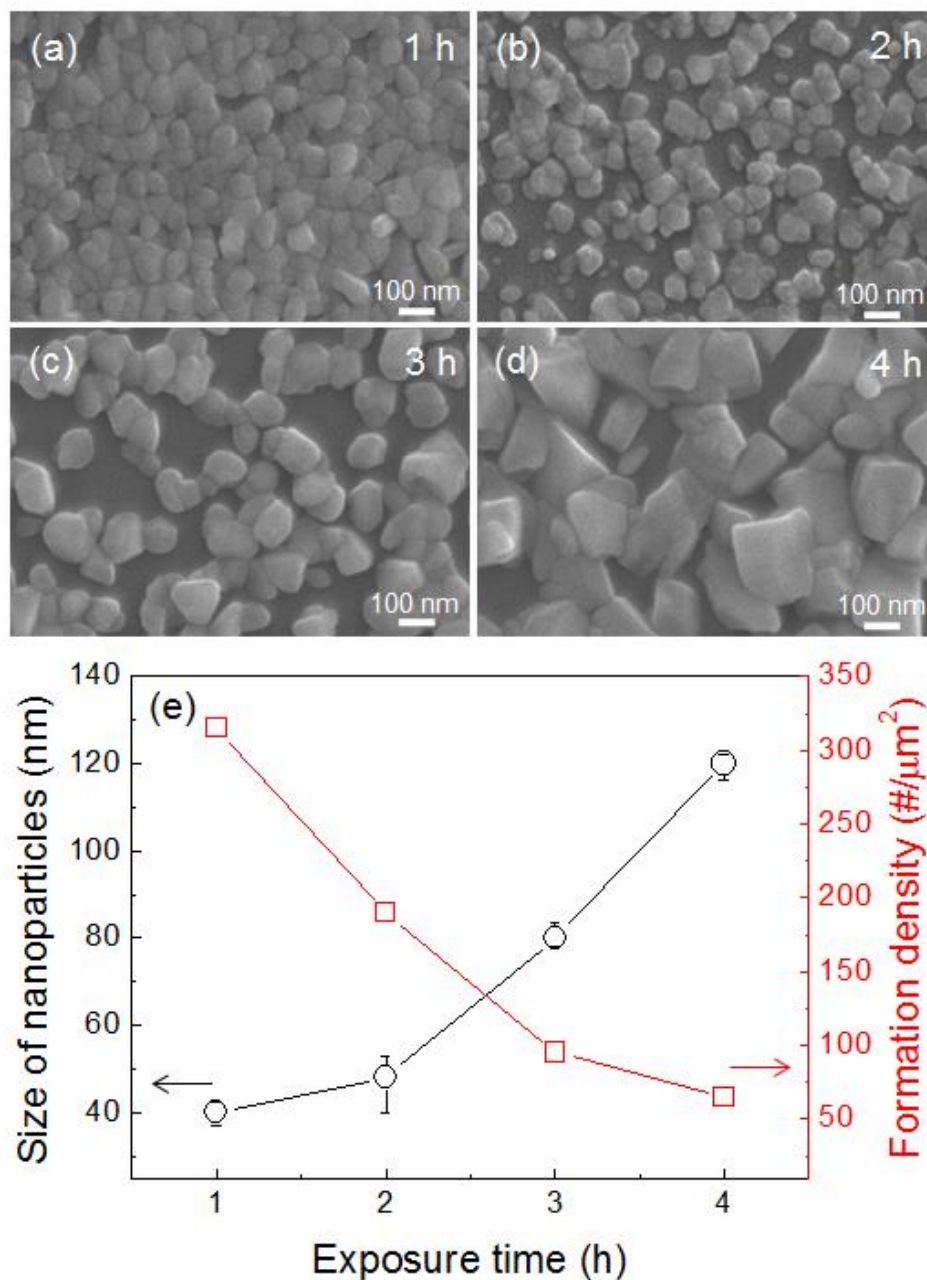


Fig. S3. Microstructures of Cu nanoparticles synthesized for various exposure times at $10 \text{ kGy}\cdot\text{h}^{-1}$ γ -ray and $0.96 \text{ mM CuSO}_4\cdot 5\text{H}_2\text{O}$: (a) 1, (b) 2, (c) 3, and (d) 4 h. (e) The size and formation density of Cu nanoparticles summarized from the microstructures in (a)–(d).